Fatigue of Engineering Materials and Structures Vol. 1, pp. 231–246
Pergamon Press. Printed in Great Britain.
Fatigue of Engineering Materials Ltd. 1979.

INITIATION AND GROWTH OF CRACKS IN BIAXIAL FATIGUE

M. W. BROWN and K. J. MILLER
Department of Mechanical Engineering, University of Sheffield,
Mappin Street, Sheffield S1 3JD, U.K.

(*Received* 2 *January* 1979)

Abstract—Observations of fatigue crack growth in smooth specimens under biaxial loading are reviewed, with particular reference to the Stage I to Stage II and Stage II to Stage I transitions. Further results are presented for 1% Cr–Mo–V steel and AISI 316 stainless steel at various temperatures, showing that all cracks may be classed as either Stage I or Stage II. Predictive criteria are suggested for the type of crack obtained, and the mechanisms for elevated temperature crack initiation are discussed.

Nomenclature

a	Crack length
K_I, K_{II}, K_{III}	Stress intensity factors for Modes I, II and III
K_{eff}	Effective stress intensity factor
α	Constant
β	Crack angle
γ	Engineering shear strain
γ_{max}	Maximum shear strain
γ_0	Surface torsional strain
Δ	Range of strain
ε	Axial strain
ε_1, ε_2, ε_3	Principal strains
ε_p	Plastic strain
λ	Strain state, $\Delta\gamma/\Delta\varepsilon$
μ	$4\tau^2/\sigma_a^2$
ν	Poisson's ratio
σ	Maximum tensile stress
σ_1	Normal stress across Stage I crack
σ_2	Normal stress across Stage II crack
σ_a	Axial stress amplitude
τ	Torsional stress amplitude
τ_1	Shear stress across Stage I crack
ϕ	Maximum shear stress
ψ	Inclination of principal strain axis

INTRODUCTION

IN UNIAXIAL fatigue tests, cracks have been observed to initiate and grow on maximum shear planes, starting from the free surface of smooth specimens and eventually turning through 45° to propagate along the plane normal to the applied load. The fatigue lifetime may therefore be roughly divided into four phases: (i) nucleation of a fatigue crack (defined as

initiation); (ii) growth on a plane of maximum shear; (iii) propagation normal to the tensile stress; and (iv) final rupture of the specimen. Phases (ii) and (iii) have been designated as Stage I and Stage II propagation respectively by Forsyth [1].

Although considerable attention has been paid to the uniaxial test, there has been comparatively little research into the effects of biaxial stresses on fatigue crack propagation [2]. Previous work is reviewed below, and further experimental results are presented to illustrate the influence of strain state on the mode of crack growth. The results are of particular importance to practical design work, cumulative damage studies and situations where the principal stress axes can rotate.

REVIEW

There are a number of conflicting theories concerning the cause of the Stage I to Stage II transition, which are briefly reviewed below. Some of these may be disproved by the occurrence of a Stage II to Stage I transition. The planes on which Stage I and Stage II cracks grow are illustrated in Fig. 1 for several of the biaxial loading situations discussed in the present work. The shaded area represents the surface plane whose position is identical in the first three columns of Fig. 1. The final column of Fig. 1 indicates the crack directions on the surface of the element considered.

Parsons and Pascoe [3] have published extensive observations of crack growth in cruciform specimens. They have shown that low cycle fatigue crack propagation occurs principally on or close to Stage I or Stage II planes, Stage I growth being dominant in the shear and plane strain tests prior to fatigue failure. One apparent exception was found in QT 35 steel with a principal strain ratio of $-\frac{1}{2}$, where short cracks initiated at 55 and 125° to the major strain axis. Nevertheless, since Poisson's ratio tends to 0·5 in low cycle fatigue, this case corresponds to the uniaxial test, and the cracks may be said to have formed on Stage I planes of maximum shear inclined to the specimen surface as shown in Fig. 1 (see also Discussion).

They also observed that in shear tests at low strain ranges on AISI 304 stainless steel, the cracks bifurcated at each end, to form two pairs of Stage II cracks, although the transition occurred fairly late in life. Zachariah [4] found similar behaviour in torsion tests on mild steel tubes, and he related the transition to the instant of crack penetration through the specimen wall. The transition could also be delayed by raising the applied stress range.

Havard and Topper [5, 6], testing thin-walled tubes with internal/external pressure and axial load, produced predominantly Stage II cracking in mild steel, except in torsion tests. They reported a few cracks parallel to the maximum principal stress direction when the strain ratio was 1·21, which they attributed to the influence of anisotropy. But one should also note that this was close to the equibiaxial state (strain ratio 1·0) where cracks may intersect the surface plane in all directions (Fig. 1). Ohji *et al.* [7–9] found that propagation could still be classified as Stage I or II in anisotropic materials, although material properties influenced which mode was favoured. In anticlastic bending, Stage I growth was always preferred.

The majority of biaxial studies have been based on the combined torsion and tension (or bending) tests, which are summarised in the following paragraphs. In low cycle fatigue, Liddle and Miller [10] obtained cracks close to the maximum shear planes except for uniaxial loading. On the other hand, Taira *et al.* [11] observed Stage II cracking in low carbon steel at 450°C. But later tests at room temperature [12] confirm the results of

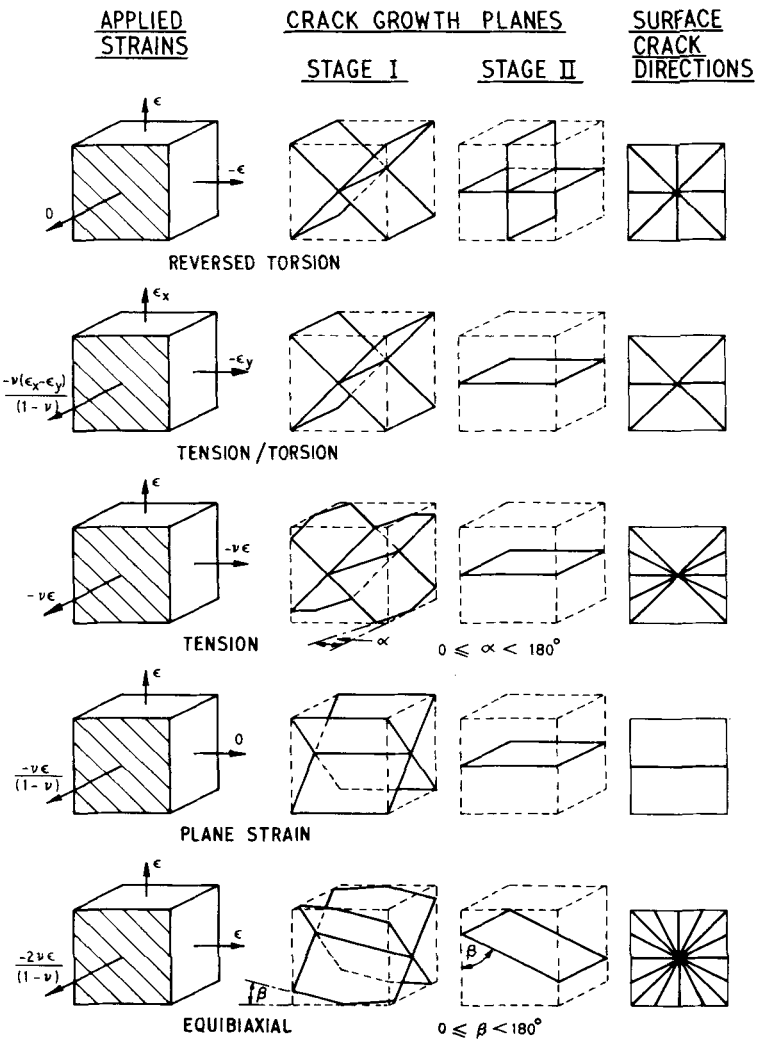

Fig. 1. Crack growth planes in biaxial systems (free surface cross-hatched).

Liddle and Miller. Kanazawa *et al.* [13] found "Stage I" cracking under out-of-phase loading, i.e. cracks initiated on those planes experiencing the greatest range of shear strain, irrespective of the rotating principal stress axes.

In high cycle fatigue studies, Gough *et al.* [14] measured the crack directions, and although they failed to find any consistent tendency in steels, Stage II failures occurred in all their tests on cast irons. However by using specimens with a considerably reduced stress concentration Findley [15] did manage to obtain consistent results for combined bending and torsion of 76S-T61 aluminium alloy. All the cracks initiated on Stage I shear planes, with a transition to Stage II growth for favourable stress states. He proposed a condition for stable Stage I propagation, that "as long as (a) the alternating principal shear stress and (b) the ratio of the alternating principal shear stress to the maximum principal stress are

larger than a certain value, the cracks continue to propagate as shear cracks". This condition was also applied to mean stress tests, predicting no effect of mean shear stresses while both a mean tensile stress and reduced stress amplitudes favoured an earlier transition to Stage II.

The studies of Cox and Field [16] using square section bars of mild steel highlighted and influence of the state of stress on crack propagation mode, since the regions of maximum shear stress and tensile stress were separated on the specimen surface. They showed clearly that "cracks starting in tension tend to follow the plane of maximum tension well into regions of high shear and similarly, that cracks starting in shear do not readily deviate into the plane of maximum tension. The tendency to persist on the plane of formation seems to be stronger for a shear crack than a tensile one, tensile cracks persisting down to about $\sigma/\phi = 1{\cdot}5$ only, whereas shear cracks occasionally persist up to $\sigma/\phi = 1{\cdot}7$ or even higher", where σ/ϕ is the ratio of the maximum tensile and shear stress. Using Forsyth's more recent terminology, their results demonstrated that once the critical σ/ϕ ratio had been passed, all Stage I cracks propagating out of the high shear strain region changed to the Stage II mode, and vice versa. So here again, the mode of crack growth was determined by the state of stress. Frost *et al.* [17] report further work by Field which gave similar behaviour in copper, but failed to obtain stable Stage I growth in high strength wrought aluminium alloys. Frost also states that under combined stress systems, the preferred direction of crack growth is Stage II. Although this statement may be valid for low ductility metals, it cannot apply to the more ductile mild steel and copper which exhibited a preference for Stage I shear, particularly evident from the above Stage II to Stage I transition. A further example of preferential Stage I growth in RR58 aluminium alloy, in spite of the influence of a notch, has been reported by Hopper [18].

The cause of the Stage I–Stage II transition has been associated with microstructural features such as grain boundaries, but this need not necessarily be the sole cause [19]. Klesnil and Lukas [20] observed the transition in single crystals of copper at a shear crack length of 0·4 mm. However Plumbridge and Ryder [19] suggested that the transition was due to a decrease in the ratio τ/σ at the crack tip resulting from movement away from the free surface, τ and σ being the shear and tensile stresses respectively. This would appear to be linked to the observation that Stage I growth only occurs close to the surface [21], and consequently the transition is precipitated at a critical depth [22]. These conclusions are probably based on uniaxial test results alone, since they do not appear to hold for the biaxial tests previously quoted.

EXPERIMENTAL OBSERVATIONS

Fatigue tests were carried out on 1% Cr–Mo–V steel and AISI 316 stainless steel at various temperatures and strain rates, given in Table 1. A description of these materials and the fatigue results are given in [23], and the fatigue machine is described elsewhere [13, 24]. Combined axial and torsional strains were applied to tubular specimens of gauge length 25 mm and internal and external diameters 16 and 22 mm respectively. On completion of a test multiple cracking was observed in this large area of uniform strain, with cracks in various stages of development including one or two large enough to have produced failure. Examination of some 69 failed specimens enabled an assessment to be made of the development of fatigue cracks under various conditions of strain state, strain rate and temperature. All tests fell within the low cycle fatigue regime.

Table 1. Test programme

Series	Material	Temperature (°C)	Shear strain rate (ks^{-1})
1	1% Cr–Mo–V	20	1·5
2	1% Cr–Mo–V	565	1·5
3	1% Cr–Mo–V	565	0·15
4	AISI 316	400	1·5

The orientation of a number of small cracks on each specimen was measured using a toolmakers microscope with a goniometer head. Larger cracks that propagated after fatigue failure, which was defined as the instant of load instability, were not studied. The results are presented graphically in Fig. 2, showing the full range of scatter measured. The crack angle is plotted against the strain state function ψ, where

$$\psi = \tfrac{1}{2} \tan^{-1} (2\lambda/3), \tag{1}$$

λ being the ratio of torsional and axial strains. We may derive equation (1) from Mohr's circle of strain, Fig. 3, containing the angle 2ψ, where ψ is the inclination of the maximum principal strain axis to the specimen axis. By Pythagoras' theorem, we obtain:

$$\tan (2\psi) = \gamma_0 / \sqrt{\gamma_{max}^2 - \gamma_0^2}, \tag{2}$$

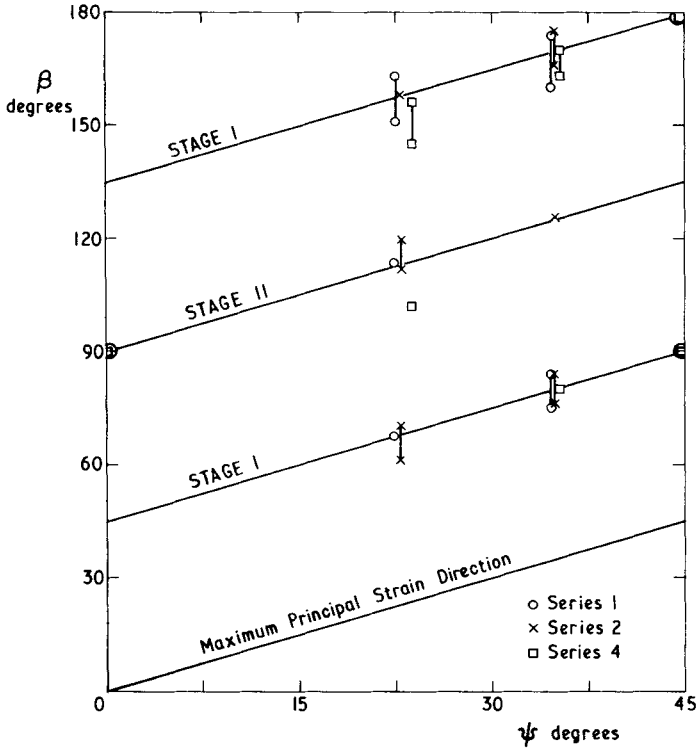

Fig. 2. Fatigue crack angles.

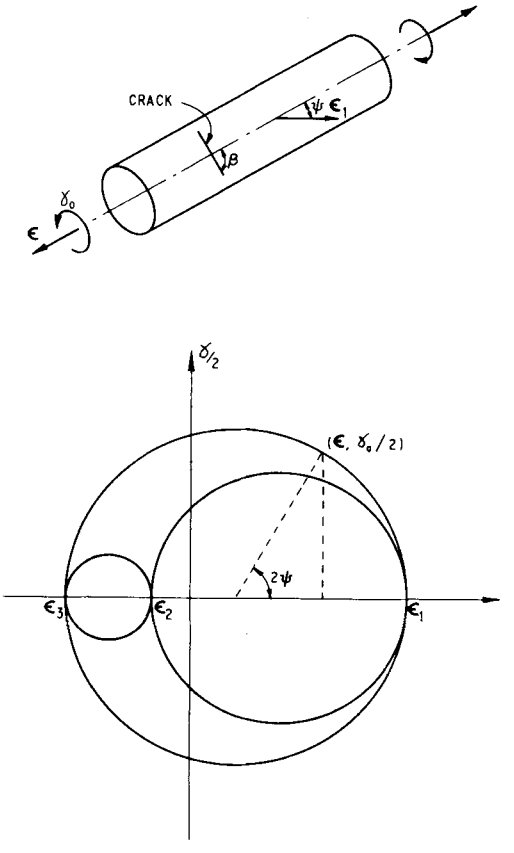

Fig. 3. Mohr's circle of strain.

where γ_0 is the torsional strain on the specimen's external surface and γ_{max} is the maximum shear strain, the diameter of the largest circle. An elastic–plastic stress analysis [25] gives:

$$\gamma_{max} = \sqrt{\gamma_0^2 + \alpha\varepsilon^2}, \tag{3}$$

where ε is the axial strain and $(1+\nu)^2 \leqslant \alpha \leqslant 2{\cdot}25$. Here ν is Poisson's ratio. Equations (2) and (3) reduce to equation (1) if ν is taken as 0·5. The errors involved in this assumption are too small to be noticeable in Fig. 2.

Comparison of the theoretical directions of crack propagation in Fig. 2 shows that the cracks followed closely the Stage I and II planes. The one exception was AISI 316 (Series 4) with $\lambda = 1{\cdot}5$ ($\psi = 22{\cdot}5$). These specimens, machined from drawn bar, exhibited a degree of anisotropy [25], which was almost certainly the cause of the deviation since Liddle and Miller [10] observed the same effect in 1% Cr–Mo–V steel drawn bar. However, the bainitic steel used in Series 1 and 2 was carefully heat treated to give isotropic properties, resulting in more confident predictions of crack orientations.

The planes and directions of crack growth depicted in Fig. 1 are based on the theory for multiaxial crack growth proposed by Brown and Miller [26]. For combined tension and torsion tests, all states of strain are classed as case A, and therefore only case A

Table 2. Crack initiation planes and propagation modes

Test series	λ	Initiation site	Propagation mode Major cracks	: Subsidiary
1. Cr–Mo–V	∞	Stage I plane	Stage I	
20°C	4·0	Stage I plane	Stage I	
	1·5	Stage I plane	Stage I	(Stage II†)
	0	Stage II‡ plane	Stage II‡	
2. Cr–Mo–V	∞	Diamond pits§	Stage I	
565°C	4·1	Diamond pits	Stage I‖	Stage II‖
	1·54	Furrow pits	Stage II	(Stage I†)
	0	Furrow pits	Stage II	
3. Cr–Mo–V	∞	Diamond pits§	Stage I	
565°C (slow)	0	Furrow pits	Stage II	Axial††
4. AISI 316	∞	Stage I plane	Stage I	
400°C	4·3	Stage I plane	Stage I	
	1·65	Stage I plane	Stage I	Stage II
	0	Stage II‡ plane	Stage II‡	

† At high strains only, $\Delta\gamma_{max} > 3\%$.
‡ Crack growth from surface defects or bore honing marks.
§ Classical Stage I initiation for $\Delta\gamma > 3{\cdot}6\%$.
‖ Major cracks Stage II with subsidiary Stage I at lower strain, $\Delta\gamma_{max} < 1{\cdot}2\%$.
†† A few short pits in the axial direction (normal to Stage II) for $\Delta\varepsilon > 1\%$.

propagation will be discussed in the remainder of the paper. The lines of intersection of the crack planes with the free surface in Fig. 1 give the crack angles plotted in Fig. 2. It is apparent that for any one specimen up to three sets of cracks may appear, as was observed on some specimens.

The modes of crack propagation are listed for each state of strain in Table 2. The Stage I–Stage II transition occurred at a λ ratio of about 1·5 in Series 1 and 4, which corresponds to $\lambda = 1{\cdot}3$ found by Cox and Field [16] in mild steel, and $\lambda \simeq 3$, observed by Findley [15] in aluminium alloy. However, in Series 2, cracks were initiated by oxidation on Stage II planes for all states of strain, which enabled a transition from Stage II to Stage I to occur for λ values greater than about 4. In mild steel at room temperature, Cox and Field obtained a λ value of 2·2 for the II to I transition. Table 2 also shows that transition depends not only on the strain state, λ, but also on the strain amplitude, higher ranges making a transition more likely.

CRACK GROWTH OBSERVATIONS

The test series fall conveniently into two groups: (i) Series 1 and 4 where corrosion had no apparent effect; and (ii) Series 2 and 3 where cracks were initiated by oxidation mechanisms. Group (i) exhibited the classical Stage I and II propagation modes discussed in the review. Figure 4 illustrates a network of orthogonal Stage I cracks typical of higher λ values. As the axial strain component was increased, reducing λ, Stage II cracks appeared, becoming dominant in the uniaxial test. These were presumably initiated on shear planes, with the exception of those cracks formed at honing marks in the specimen bore.

For group (ii) an entirely different mechanism of initiation was encountered. The torsional and uniaxial tests are now discussed in detail, but for intermediate strain states a mixture of these two cases was observed as shown in Table 2. Similar crack growth has been reported by both Gardiner [27] and Weerasooriya [28] in pure shear studies.

(a) *Torsion tests*

During the initial heating up period of about one hour, a thin protective oxide layer formed on the specimen surface, which was cracked in a brittle manner on the first strain cycle, normal to the principal axes. Having broken this protective film, oxidation and surface deterioration could occur rapidly under each oxide crack, since it was re-opened in each succeeding cycle. Deep layers of oxide were gradually built up around each initial crack, as shown in Fig. 5. These oxide layers formed square pyramids with the initial cracks lying along the two diagonals at 45° to the specimen axis. A remarkable feature of the damage was that the pyramids were arranged in two straight lines in a regular network, these lines following the principal shear directions, often up to 5 mm in length (Fig. 5). Removal of the oxidation revealed rows of pits underneath, each being reminiscent of a diamond pyramid indentation (Fig. 6). As these "diamond pits" deepened with further cycling, fatigue cracks formed along the two diagonals and propagated as Stage II cracks. Since the pits had already formed in long lines, fatigue cracks in adjacent pits were able to link up to produce a long zig-zag crack (Fig. 7). On reaching a certain depth, this macroscopic crack turned to a Stage I shear plane, and conventional torsional crack growth continued until failure. Thus a transition occurred from Stage II propagation to Stage I.

The depth of pitting and crack growth at the II to I transition was considerably greater in the Series 3 tests, which were conducted at a lower strain rate. The oxide layer was much thicker at the conclusion of these tests, due to the rather longer time spent at temperature.

For tests at higher strain ranges ($\Delta\gamma > 4\%$) crack initiation followed the normal Stage I planes, typical of room temperature tests, as shown in Fig. 8 which illustrates an orthogonal network of cracks. Presumably in this case, conventional crack initiation mechanisms were faster than the oxidation process for these high strain ranges.

(b) *Uniaxial tests*

In the uniaxial tests, the protective oxide layer was again broken in the first cycle, producing long, straight circumferential cracks. Pits developed under these oxide cracks and long ridges of oxide were built up with the repeated opening of the oxide film in the tensile portion of each cycle (Fig. 9). The pits below the oxide layer were uniformly spaced on parallel Stage II planes (Fig. 10), giving the specimen surface some resemblance with the furrows of a ploughed field. The bottom of each "furrow pit" produced a sharp stress concentration from which a Stage II fatigue crack propagated through the wall thickness, sometimes leaving striation markings visible through the heavy oxidation.

In low strain rate tests, a few short axial pits were observed at high strain ranges. They were presumably formed when brittle oxide cracks were opened during the compressive half of the cycle, normal to the minor principal surface strain.

However, for the Series 3 test at the lowest strain range tested (0·5%) the strain was too low to fracture the protective oxide layer, so that it remained comparatively thin and no pitting or fatigue cracking was observed over much of the gauge area. Failure occurred at the end of the gauge length, where corrosion damage was intensified due to the strain concentration [29].

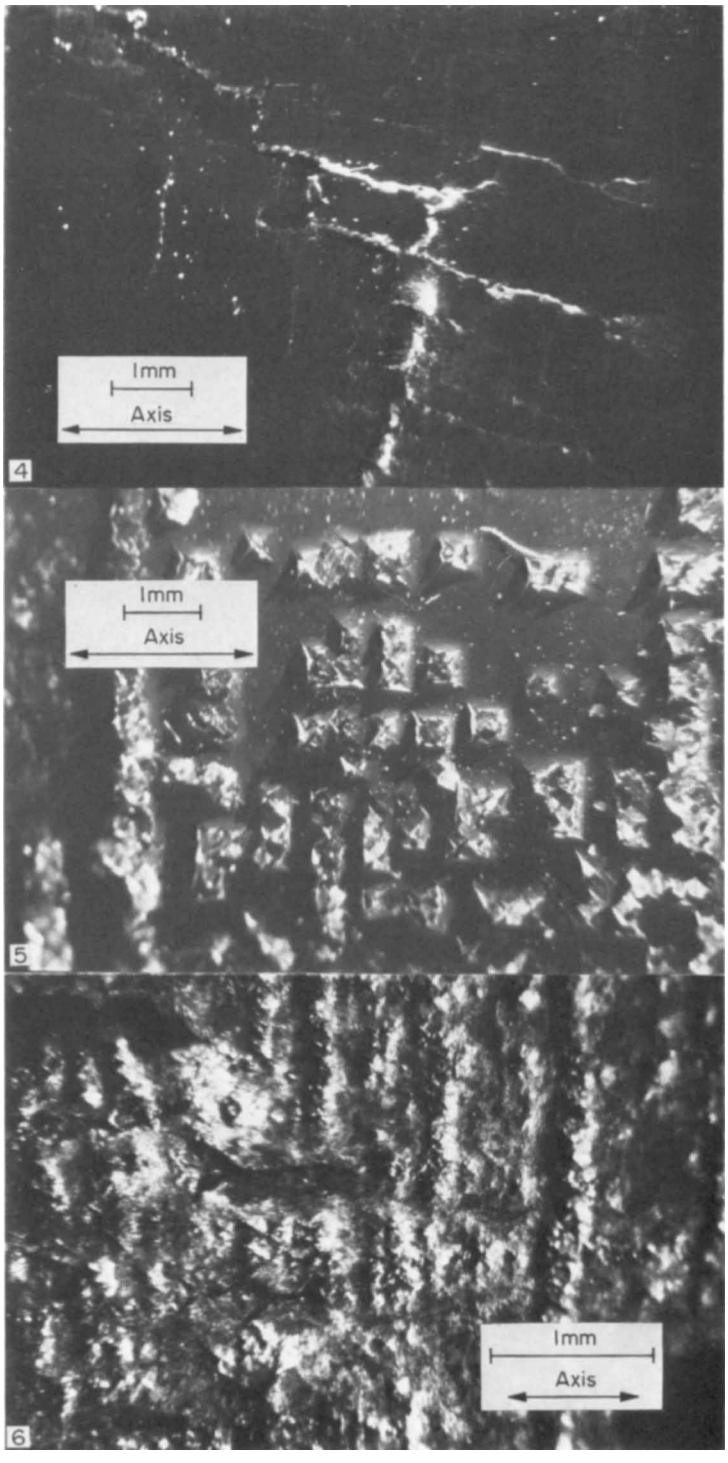

Fig. 4. Stage I cracking. Series 1, $\lambda = 4$, $\Delta\gamma_{max} = 1{\cdot}78\%$.
Fig. 5. Oxide formation in torsion. Series 3, $\Delta\gamma = 1{\cdot}98\%$.
Fig. 6. Oxide pits and cracks in torsion. Series 2, $\Delta\gamma = 1{\cdot}14\%$.

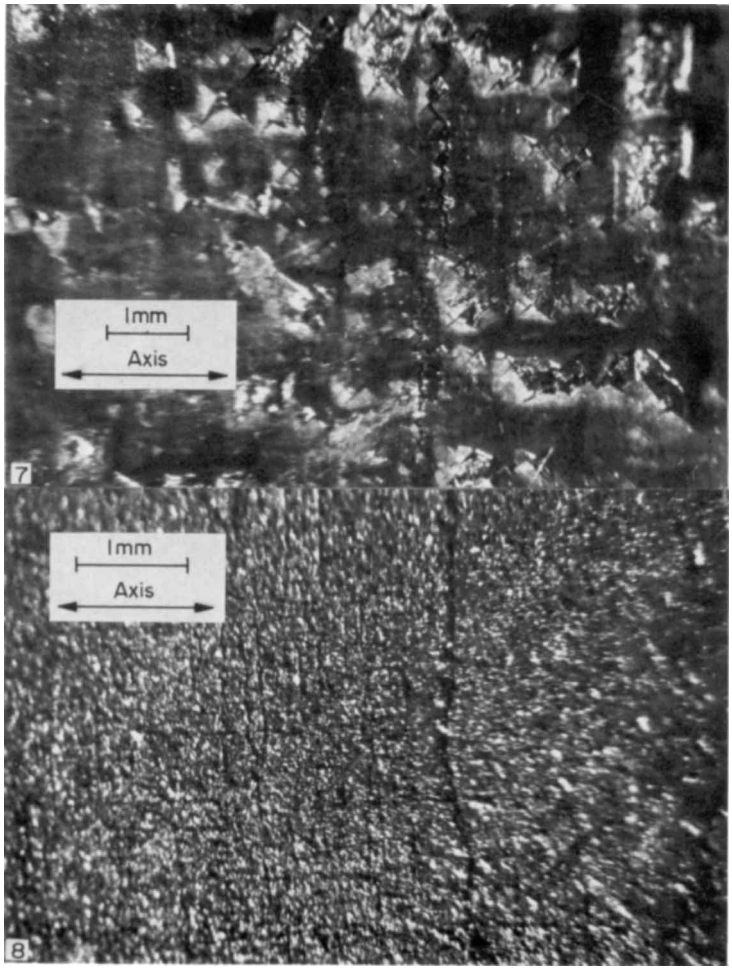

Fig. 7. Torsional zig-zag cracks. Series 2, $\Delta\gamma = 1{\cdot}75\%$.
Fig. 8. Torsional Stage I cracking. Series 2, $\Delta\gamma = 7{\cdot}8\%$.

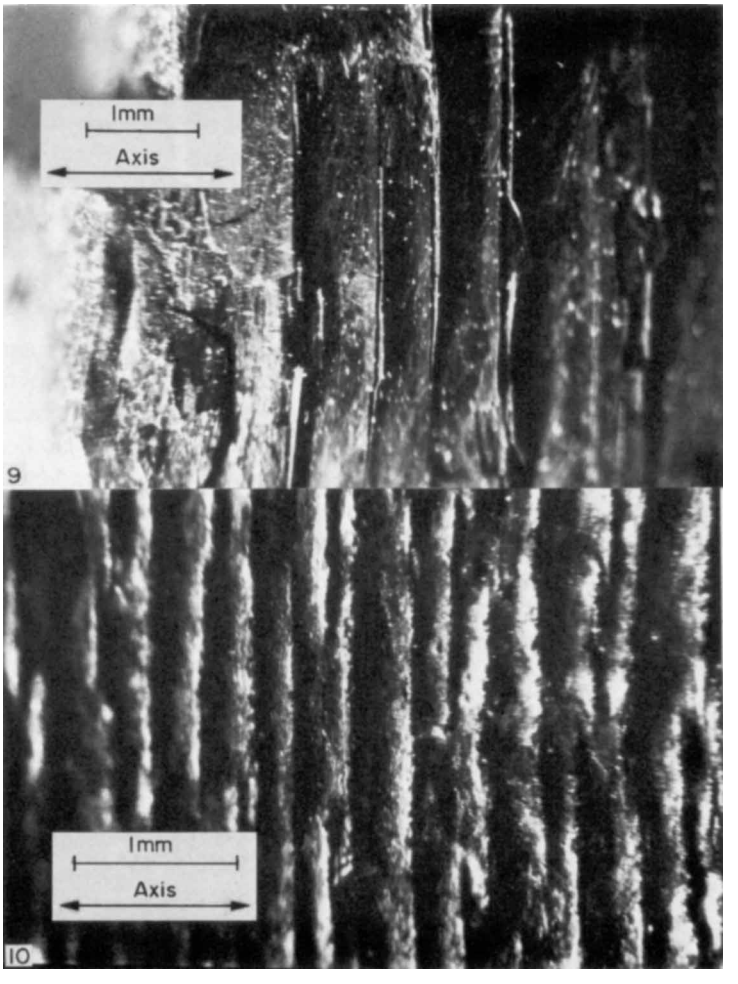

Fig. 9. Uniaxial oxide formation. Series 3, $\Delta\varepsilon = 0{\cdot}51\%$.
Fig. 10. Uniaxial pitting. Series 3, $\Delta\varepsilon = 0{\cdot}71\%$.

In both torsional and uniaxial tests, the pits were more widely spaced at lower strain ranges. The mechanisms of initiation and propagation are summarised in Table 2 for all of the strain states. The subsidiary propagation mode refers to small amounts of cracking in a second mode observed in certain tests.

DISCUSSION

For both the uniaxial and the torsional tests at 565°C, the mechanism of initiation is reasonably clear. Fracture of the external oxide layer led to localised oxidation, pitting, and Stage II fatigue crack growth from the resulting notches. However, for sufficiently high λ values, a transition to a Stage I propagation mode occurred. Reduction of the strain rate greatly accelerated both initiation and propagation, due to the interaction of cyclic strain and oxidation [23].

This simple mechanism fails to explain the regular pattern of pitting, since one might expect pits to develop in a random manner. A possible mechanism for the observed brittle cracking pattern in torsion is related to the cyclic softening behaviour of the steel. Preferential regions of intense deformation, similar to Luder's bands, may form with cyclic softening of the specimen, a transient effect associated with low strain hardening exponents. In the first cycle, discrete regions may experience slightly higher strains than the average. In the second cycle, those regions may be softer, and therefore they experience even higher strains in order to maintain equilibrium with the applied load. This effect builds up in the third and subsequent cycles due to the unstable situation of a decreasing stress range with increasing strain, producing Luder's bands which are aligned with maximum shear planes (Fig. 11). Since the major part of deformation is concentrated in these bands, the brittle cracking of the oxide layer is also confined, producing the long straight lines of pyramids observed. At higher strain ranges, more Luder's bands are produced, so that the pits are smaller and closer together, again as observed.

Luder's bands may also form in the uniaxial tests (Fig. 11), but since the degree of softening was less in uniaxial tests [24, 25], long straight pits were able to form without being confined to a single band. Analysis of the applied strain ranges revealed that the oxide layer fractured when the maximum principal strain amplitude exceeded 0·25%, below which fatigue life was considerably extended [23]. However in torsion, the strain localisation in Luder's bands reduced the mean critical principal strain over the gauge length to below 0·19%, with a consequent reduction in fatigue life.

The transition from Stage I to Stage II propagation in ductile metals appears to be related to the applied strain state rather than crack length. In the Appendix, a fracture mechanics argument is employed to derive the critical stress state for this transition. Although such analysis is only applicable to small scale yielding around crack tips, the theoretical transition values agree surprisingly well with the experimental values of Cox and Field, and those presented here for low cycle fatigue. However, the most interesting conclusion to be drawn from the analysis is that crack length does not influence the transition. Instead, it is dependent on the applied stress state, a point brought out in the review above.

It is pertinent to consider why the short cracks observed by Parsons and Pascoe [3] in the uniaxial test, formed only at 55 and 125° to the loading axis. One might expect a general distribution of Stage I cracks intersecting the surface at all angles between 45 and 135°. If one assumes that the cracks initiate only in ferrite grains (b.c.c.) a possible explanation is

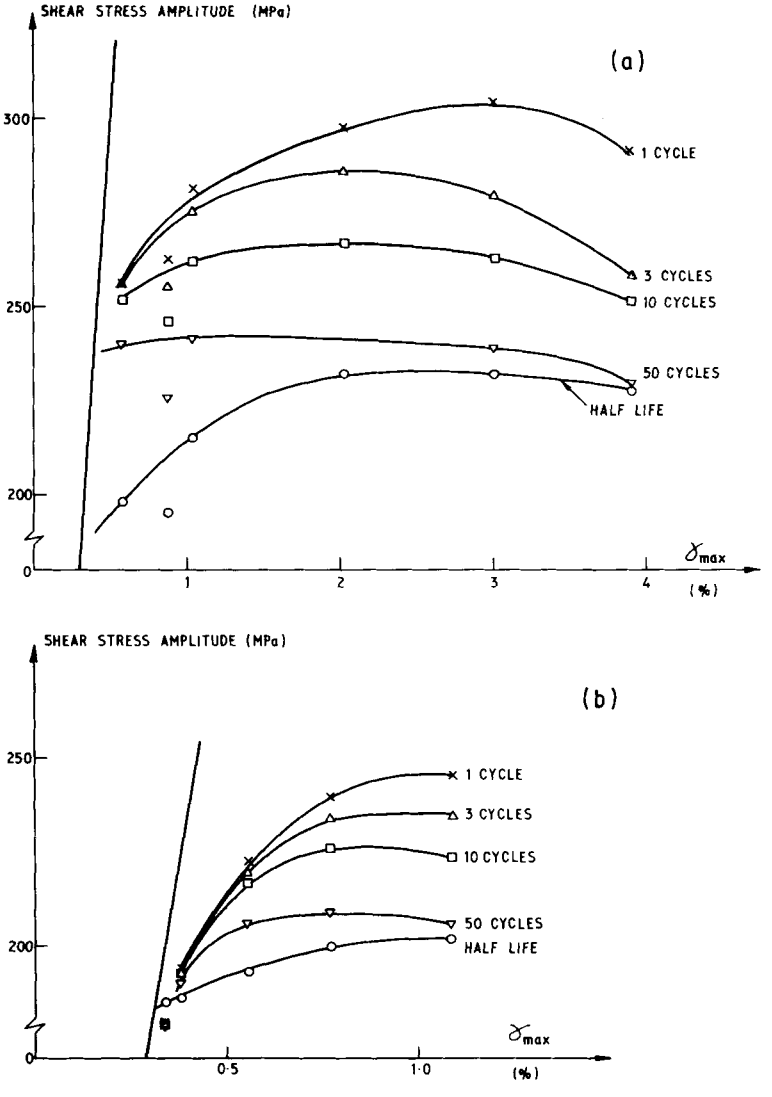

Fig. 11. Cyclic softening curves. Series 2: (a) Torsional cycling; (b) Axial cycling.

that the initiation mechanism is favoured by those grains with a $(0, \bar{1}, 1)$ surface plane and with the [1, 0, 0] direction aligned with the tensile axis. In this case the crack intersects the surface at an angle of 55°.

CONCLUSIONS

(1) At room temperature, fatigue cracks initiate on Stage I planes. A transition to Stage II propagation occurs for strain state ratios below 1·5.

(2) At high temperature in an oxidising environment, fatigue cracks initiate from pits

and grow on Stage II planes. A transition to Stage I propagation occurs for strain state ratios above 4.

Acknowledgements—We gratefully acknowledge the support and assistance of the Science Research Council, Emmanuel College, Cambridge, and the University of Illinois Department of Theoretical and Applied Mechanics. The experimental work was conducted at the Cambridge University Engineering Department, using materials that were donated by the Central Electricity Generating Board.

REFERENCES

[1] Forsyth, P. J. E. 'A two stage process of fatigue crack growth', Proc. Crack Propagation Symp., Cranfield 1961, pp. 76–94.
[2] Miller, K. J. 'Fatigue under complex stress', *Metal Sci.* 1977 **11,** 432–438.
[3] Parsons, M. W. and Pascoe, K. J. 'Observations of surface deformation, crack initiation and crack growth in low-cycle fatigue under biaxial stress', *Mater. Sci. Engng* 1976 **22,** 31–50.
[4] Zachariah, K. P. 'Fatigue crack initiation and Stage I propagation', Ph.D. Thesis, University of Cambridge 1974.
[5] Havard, D. G. and Topper, T. H. 'New equipment for cyclic biaxial testing', *Expl Mech.* 1969 **9,** 550–557.
[6] Havard, D. G. and Topper, T. H. 'Low cycle biaxial fatigue of AISI 1018 steel', *Ont. Hydro Res. Q.* 1969 **21** (2), 1–12.
[7] Ohji, K., Ogura, K., Harada, S. and Senga, H. 'Biaxial low-cycle fatigue of anisotropic rolled steel plates', *Bull. J.S.M.E.* 1974 **17,** 32–40.
[8] Ohji, K., Ogura, K. and Harada, S. 'Observations of fatigue crack propagation in an anisotropic rolled steel plate', Technology Reports of Osaka University 1974 **24,** 2.
[9] Ohji, K., Ogura, K. and Harada, S. 'Observation of low cycle fatigue crack initiation and propagation in anisotropic rolled steel under biaxial stressing', *Bull. J.S.M.E.* 1975 **18,** 17–24.
[10] Liddle, M. and Miller, K. J. 'Multiaxial high strain fatigue', 3rd Int. Conf. Fracture, Munich 1973.
[11] Taira, S., Inoue, T. and Takahashi, M. 'Low cycle fatigue under multiaxial stresses (in the case of combined cyclic tension-compression and cyclic torsion in the same phase at elevated temperature)', Proc. 10th Japan Congress on Testing Materials 1967, pp. 18–23.
[12] Taira, S., Inoue, T. and Yoshida, T. 'Low cycle fatigue under multiaxial stresses (in the case of combined cyclic tension-compression and cyclic torsion at room temperature)', Proc. 12th Japan Congress on Materials Research 1969, pp. 50–55.
[13] Kanazawa, K., Miller, K. J. and Brown, M. W. 'Low-cycle fatigue under out-of-phase loading conditions', *Trans. Am. Soc. mech. Engrs, J. Engng Mat. Tech.* 1977 **99** (H), 222–228.
[14] Gough, H. J., Pollard, H. V. and Clenshaw, W. J. 'Some experiments on the resistance of metals to fatigue under combined stresses', Aeronautical Research Council, R. and M. 2522, 1951.
[15] Findley, W. N. 'Combined-stress fatigue strength of 76S–T61 aluminium alloy with superimposed mean stresses and corrections for yielding', NACA Tech. Note 2924, 1953.
[16] Cox, H. L. and Field, J. E. 'The initiation and propagation of fatigue cracks in mild steel pieces of square section', *Aeronaut. Q.* 1952 **4,** 1–18.
[17] Frost, N. E., Marsh, K. J. and Pook, L. P. "Metal Fatigue". Clarendon Press, Oxford, 1974, pp. 269–270.
[18] Hopper, C. D. 'Fatigue crack propagation under biaxial stresses', Ph.D. Thesis, University of Cambridge 1976.
[19] Plumbridge, W. J. and Ryder, D. A. 'The metallography of fatigue', *Metall. Rev.* 1969 **14,** 119–142.
[20] Klesnil, M. and Lukas, P. 'Dislocation substructure associated with propagating fatigue crack', 2nd Int. Conf. Fracture, Brighton 1969, pp. 725–730.
[21] Beardmore, P. and Feltner, C. E. 'Cyclic deformation and fracture characteristics of a low carbon martensitic steel', 2nd Int. Conf. Fracture, Brighton, 1969, pp. 607–619.
[22] Feltner, C. E. and Beardmore, P. 'Strengthening mechanisms in fatigue', Am. Soc. Test. Mater. STP467, pp. 77–112, 1970.

[23] Brown, M. W. and Miller, K. J. 'High temperature low cycle biaxial fatigue of two steels', *Fatigue Engng Mater. Struct.* 1979 **1.**
[24] Brown, M. W. 'High temperature multiaxial fatigue', Ph.D. Thesis, University of Cambridge, 1975.
[25] Brown, M. W. and Miller, K. J. 'Biaxial cyclic deformation behaviour of steels', *Fatigue Engng Mater. Struct.* 1979 **1,** 93–106.
[26] Brown, M. W. and Miller, K. J. 'A theory for fatigue failure under multiaxial stress–strain conditions', *Proc. Instn mech. Engrs* 1973 **187,** 745–755.
[27] Gardiner, T. 'Cumulative fatigue damage at elevated temperature', Ph.D. Thesis, University of Cambridge 1974.
[28] Weerasooriya, T. 'Fatigue under biaxial loading at 565°C and deformation characteristics of $2\frac{1}{4}\%$ Cr–1% Mo steel', Ph.D. Thesis, University of Cambridge 1978.
[29] Coffin, L. F. 'Cyclic-strain-induced oxidation of high-temperature alloys', *Trans. Am. Soc. Metals* 1963 **56,** 339–344.
[30] Tanaka, K. 'Fatigue crack propagation from a crack inclined to cyclic tensile axis', *Engng Fracture Mech.* 1974 **6,** 493–507.

APPENDIX—THE STAGE I–STAGE II TRANSITION

Tanaka [30] has derived an effective stress intensity factor, K_{eff}, for use in Paris' law in order to predict fatigue crack propagation rates. K_{eff} relates the growth due to each of the three modes of crack extension,

$$K_{\text{eff}} = [K_{\text{I}}^4 + 8K_{\text{II}}^4 + 8K_{\text{III}}^4/(1-\nu)]^{\frac{1}{4}}. \tag{4}$$

We may use this expression to find the fastest mode of crack growth, Stage I or Stage II, under case A loading with an applied axial stress, σ_a, and a shear stress, τ.

For a Stage I crack, the stresses σ_1 and τ_1 giving Mode I and Mode II crack opening respectively are given by:

$$\sigma_1 = \sigma_a/2 \tag{5}$$

and

$$\tau_1 = \sqrt{(\sigma_a/2)^2 + \tau^2}. \tag{6}$$

For case A propagation of a small crack along the surface, one may assume approximate stress intensity factors for Stage I growth, namely $K_{\text{I}} = \sigma_1\sqrt{\pi a}$, $K_{\text{II}} = \tau_1\sqrt{\pi a}$ and $K_{\text{III}} = 0$. Similarly for a Stage II crack, the stress giving Mode I crack opening is:

$$\sigma_2 = \sigma_a/2 + \sqrt{(\sigma_a/2)^2 + \tau^2}, \tag{7}$$

and the corresponding stress intensity factor is $K_{\text{I}} = \sigma_2\sqrt{\pi a}$. K_{II} and K_{III} are zero, since σ_2 is the maximum principal stress.

Solving equations (4–7) and equating the effective stress intensity factors for Stage I and Stage II growth, one obtains:

$$4(1+\mu)^{\frac{1}{2}} + 6(1+\mu) + 4(1+\mu)^{1\cdot5} - 7(1+\mu)^2 = 0,$$

where $\mu = 4\tau^2/\sigma_a^2$. Solution of this equation gives a condition for the state of stress at the Stage I–Stage II transition, $\mu = 1{\cdot}077$.

μ is simply related to λ for linear elastic behaviour by the relation

$$\lambda = \sqrt{\mu}(1+\nu).$$

With $\nu = 0{\cdot}5$ for incompressibility, $\lambda = 1{\cdot}56$, compared with the experimental value of 1·5 for low cycle fatigue. With $\nu = 0{\cdot}3$ for mild steel, $\lambda = 1{\cdot}35$ compared with the experimental value of 1·3 obtained by Cox and Field, for the I to II transition. However, the values for the II to I transition of 4 and 2·2 are not in such good agreement. The transition λ values are very sensitive to the chosen *approximate* K values, so that one cannot depend on the analysis for a rigorous solution. It serves only to demonstrate that the stable mode of crack growth depends on the applied stress or strain state.